Advanced Ceramics Progress

Research Article

Journal Homepage: www.acerp.ir

Ultraviolet Detectors Based on Annealed Zinc Oxide Thin Films: Epitaxial Growth and Physical Characterizations

M. Moghaddam [a], N. Naderi [a] *, M. Goodarzi [a]

[a] *Department of semiconductors, Materials and Energy Research Center (MERC), Karaj, Iran*

PAPER INFO

Paper history:

Received 26 October 2019
Accepted in revised form 31 December 2019

Keywords:

ZnO Thin Films
Physical Properties
Thermal Annealing
Ultraviolet Detector
Epitaxial Growth

ABSTRACT

In this report, ultraviolet (UV) detectors were fabricated based on zinc oxide thin films. The epitaxial growth of zinc oxide thin films was carried out on a bare glass substrate with a preferred orientation to (002) plane of wurtzite structure through radio frequency sputtering technique. The structural properties indicated a dominant peak at 2θ=34.28°, which was matched with JCPDS reference card No. 34-1451 and showed the wurtzite phase of deposited ZnO thin films. This peak showed the preferred orientation with the c-axis perpendicular to the surface. The crystallite size was estimated using the Scherrer equation as much as 44.5nm. The morphology of samples showed that pebble-shaped ZnO particles were covered on the entire substrate homogeneously. The results indicated the excellent optical properties in the visible-infrared region with high absorption in the UV spectrum. The extrapolated cut-off for the transmittance spectrum was at 373nm, which confirmed the calculated optical bandgap of this sample at 3.27eV. The optical properties showed that the deposited samples are suitable substrates for the fabrication of UV detectors. Two back-to-back Schottky contacts of Au were deposited on the ZnO substrate to fabricate UV detectors, and a metal-semiconductor-metal structure was designed. The optoelectrical properties of detectors were carried out using the measurement of current-voltage curves. The results indicated a high photosensitivity of 0.32 corresponding to the high performance of the fabricated device. Moreover, the device showed a short rise time of 0.40s and recovery time of 0.45s indicating the high speed of detection for fabricated UV detectors.

1. INTRODUCTION

Recently, ultraviolet detectors have attracted much attention in optoelectronic industries due to their enormous applications in flame detectors, environmental sensors, and even biological sensors [1]. Zinc oxide (ZnO) is one of the most important II-VI semiconductor materials, which has a direct bandgap (3.3eV) at room temperature. ZnO grows with hexagonal wurtzite structure (a=3.249Å and c=5.206Å), which is naturally n-type [2]. ZnO has a large excitation binding energy (60MeV), high optical transmittance (>80%) in the visible, and infrared spectrum [3]. ZnO attracted extensive attention for many applications such as transparent conductive films, acoustic waves devices, and solar cells window due to the outstanding optical, electrical and piezoelectric properties [4].
It has attracted a potential application for the fabrication of UV detectors because the optical bandgap of this semiconductor lies in the UV region [5]. Several techniques, such as chemical bath deposition (CBD), spray pyrolysis, chemical vapor deposition (CVD), and radiofrequency (RF) magnetron sputtering have been used for deposition of ZnO thin films on different substrates [6]. Among these methods, deposited layers with RF sputtering have many advantages such as good adherence to the substrate, uniformity of deposited films, stability, growth of ZnO thin films with high c-axis orientation, packing density even on amorphous substrates and the thickness of the layers in the deposition process is controllable [2,7].
A various substrate such as Si, sapphire, and glass can be used for deposition of ZnO thin film through RF sputtering technique. Among them, the glass substrate is popular due to its low cost and low roughness [8].
In this study, the ZnO thin films with a thickness of 200nm were successfully deposited on a bare glass substrate using RF sputtering technique. The surface

* Corresponding Author Email: n.naderi@merc.ac.ir (N. Naderi)

morphology and structural parameters of deposited thin films were investigated. Besides, the optical properties of the deposited layer were measured by UV-VIS analysis. Ultraviolet detectors were fabricated by the coating of Au interdigitated contacts with a thickness of 200nm on the ZnO substrate to study the application of deposited ZnO thin films. The optoelectrical properties of fabricated detectors were measured under UV radiation and in darkness.

2. EXPERIMENTAL PROCEDURES

2.1. Deposition of thin films

The glass substrates were cleaned using the ultrasonic clean method in hydrochloric acid and distilled water (1:5) for 10min to remove inorganic residues. Thereafter, they were rinsed by distilled water and ultrasonicated for 10min to remove the organic residues. This step was followed by the drying process in ambient temperature. The undoped ZnO thin films were successfully deposited on cleaned glass substrates using RF magnetron sputtering technique with a ZnO disk (99.99% purity) as a target. the vacuum chamber was pumped down to the base pressure of 6×10^{-5}mbar before deposition. The pressure of the argon gas (99.999% purity) was fixed at 6.9×10^{-3}mbar (working pressure) for deposition, and the RF power was as much as 135W. The distance between substrate and target was fixed at 6cm. The thickness of ZnO thin films reached at 200nm after 44min of deposition.

2.2. Post-deposition annealing process

A post-deposition annealing process was followed in a quartz tube furnace to improve the optical and structural properties of ZnO thin film. Post-annealing process induces crystallinity in deposited ZnO thin films. Moreover, it enhances the optical properties of these structures. The temperature was set at 200ºC and the annealing process was carried out for 1h under argon atmosphere. The samples then remained in the furnace and the cooling down process was followed until room temperature under Ar gas flow.

2.3. Fabrication of ultraviolet detectors

Two back-to-back Schottkey contacts of Au were sputtered on top of ZnO thin films to fabricate ZnO-based MSM UV-detector. An interdigitated finger-shaped pattern with a length of 2.8mm and a width of 50µm and an electrode distance of 120µm was applied using a steel mask to decrease the distance between two electrodes. The effective area of fabricated photodetector was estimated as much as 0.1cm^2. The device was then exposed to UV illumination and the current-voltage (I-V) characteristics were measured at darkness and under illumination using a computer-controlled source-meter (Keithley 2400, USA).

2.4. Characterization techniques

The structural properties of the deposited ZnO thin films were analyzed by X-ray diffraction (XRD, Philips PW3710) with Cu *Kα* radiation (λ=1.5405Å) in a 2θ range of 20°–70°. The ZnO thin film surface morphology was characterized using field emission scanning electron microscopy (FESEM, MIRA3 TESCAN). The energy dispersive X-ray analysis (EDX, TESCAN) was used to identify the elements of the deposited layer surface. The UV-VIS spectrophotometer (Perkin–Elmer Lambda 25) was employed for optical characterization in the wavelength range of 300–1000nm while the glass substrate used as the blank for this sample.

3. RESULTS AND DISSCUSSION

3.1. X-ray diffraction analysis

Fig. 1 shows the XRD pattern of deposited ZnO on a bare glass substrate. For this sample, only one peak at 2θ=34.28 was observed in the range of 20-70°. This peak diffracted from (002) plan of the ZnO based on JCPDS reference with card No. 34-1451 and shows the preferred orientation with the c-axis perpendicular to the surface substrate. The (002) peak is related to the growth of the ZnO thin films with the hexagonal structure.

The inter-planer spacing (d_{hkl}) and the average crystallite size (D) of the ZnO thin films were calculated through Bragg and Scherrer equations, respectively [9,10]:

$$n\lambda = 2d_{hkl}\sin\theta \qquad (1)$$

$$D = \frac{K\lambda}{\beta\cos\theta} \qquad (2)$$

where n is the order of diffraction, θ is the diffraction angle, λ shows the wavelength of the incident X-ray, and β and K are the full width at half maximum (FWHM) of the (002) peak and the Scherrer constant, respectively.

The lattice parameters (a) and (c) of the hexagonal phase for deposited ZnO thin films were evaluated using the following equations [11]:

$$a = \frac{\lambda}{\sqrt{3}\sin\theta} \qquad (3)$$

$$c = \frac{\lambda}{\sin\theta} \qquad (4)$$

The structural parameters of the deposited ZnO thin films in this study were compared to another report and were summarized in Table 1.

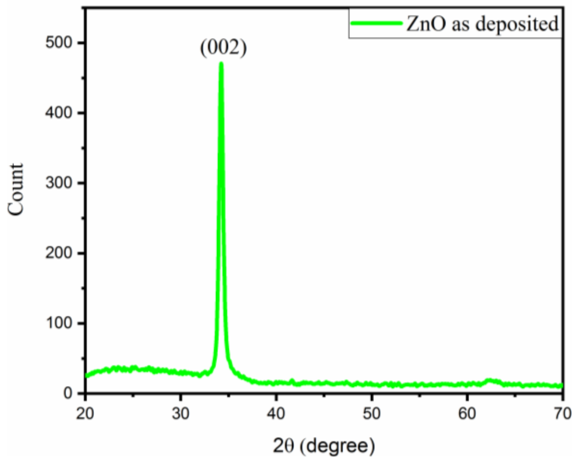

Figure 1. XRD pattern of deposited ZnO

3.2. Surface morphology

Fig. 2 (a) shows the FESEM micrograph of deposited ZnO thin film on the glass substrate using the magnetron sputtering technique. The deposited ZnO thin films show smooth, homogeneous, and uniform pebble morphology. The morphology of samples showed that ZnO pebbles are covered on the entire substrate homogeneously.

In this case, no cracks and pinholes were observed on the surface. The cross-sectional FESEM image of deposited ZnO samples was illustrated in Fig. 2 (b). It showed that a uniform ZnO thin film with a thickness of 200nm was deposited on the substrate successfully.

The mechanical tests showed that there was a good adherence between the top-layer and the substrate. The cross-sectional morphology of ZnO thin films showed no cracks and defects in this sample.

3.3. Energy dispersive X–ray analysis

Fig. 3 indicates the elemental composition of the ZnO thin films. The peaks of Zn and O can be observed in the spectrum, which is related to ZnO thin films. The Si, O, and Ca peaks are corresponding to the glass substrate.

3.4. UV–visible analysis

Fig. 4 (a) shows the UV-VIS transmittance spectrum of ZnO thin films. The sample has a high transmittance in the UV-VIS region (>80%). For the wavelengths below the 375nm, the sample does not show the transmission spectrum because in this region (300-375nm), ZnO has a high absorption coefficient.

Fig. 4 (b) illustrates the Tauc plot to obtain the optical bandgap of ZnO thin films. The transmission spectrum of this sample is used to estimate the optical bandgap (Eg) using the Tauc plot equation [12] as follows:

$$(\alpha h\upsilon) = A(h\upsilon - E_g)^n \qquad (5)$$

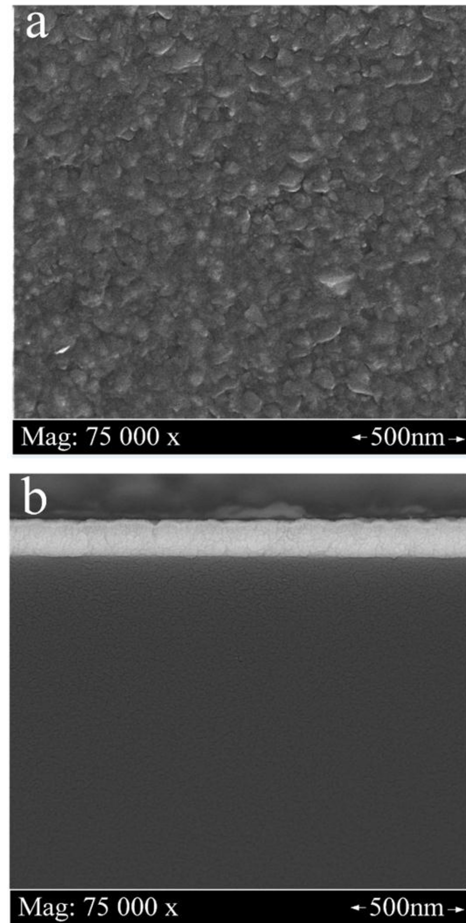

Figure 2. Planar FESEM image of deposited ZnO thin film **(a)** and cross-sectional FESEM of the samples **(b)**

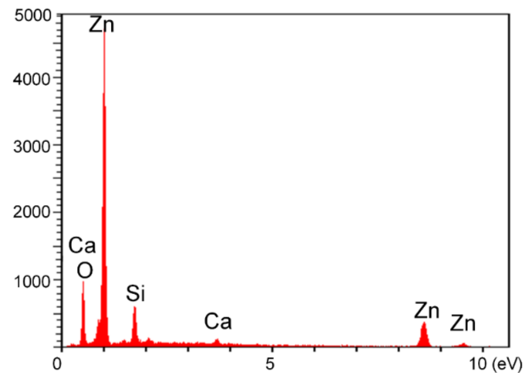

Figure 3. Energy dispersive X–ray spectrum of ZnO thin films

where α shows the absorption coefficient, $h\upsilon$ is the energy of the incident photon, A demonstrates a constant and $n=1/2$ for the direct bandgap semiconductors. The E_g values of the sample are estimated from the plots of $(\alpha h\upsilon)^2$ versus $h\upsilon$ by extrapolating of the tangent line (dotted line). The E_g value of this sample is 3.27eV, which is closed to the bandgap of bulk ZnO.

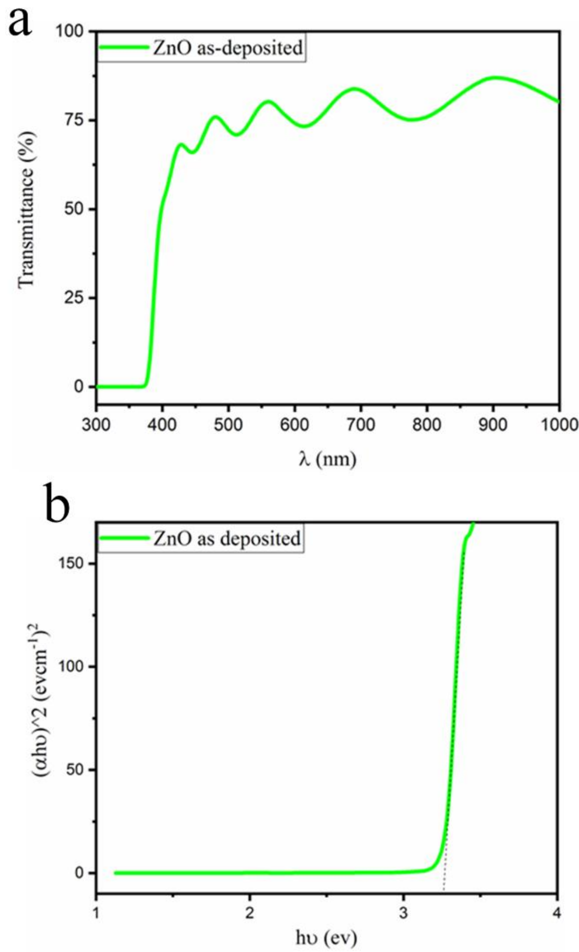

Figure 4. The transmittance spectrum of the deposited ZnO **(a)** and the calculated optical bandgap **(b)**

3.5. Optoelectrical measurements

Fig. 5 shows the current-voltage (I-V) curves for the UV detector based on ZnO thin films at darkness and under UV illumination with the wavelength of 350nm and the incident power of 1.5mW. The device indicated a high photocurrent density of 330mA.cm^{-2} under UV illumination and a low current density of 250mA.cm^{-2} at the darkness with the applied voltage of 4.5V. The nonlinear behavior of the I-V curves is related to the formation of Schottky barriers at the Au/CdS interface. Photosensitivity is an important factor in determining the quality of the sensor and is defined as the ratio of the photocurrent to the dark current, which is calculated using the following equation [13]:

$$S = \frac{I_{Ph} - I_d}{I_d} \quad (6)$$

where I_{Ph} and I_d represent the photocurrent and the dark current of photodetectors, respectively. The calculated values of sensitivity is summarized in Table 2.

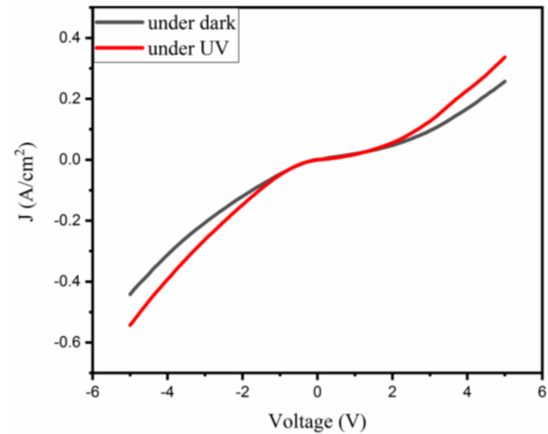

Figure 5. The current density-voltage curves of the fabricated UV detector based on ZnO thin film

The current gain (ratio of photocurrent to dark current) was calculated from I–V characteristics using the following equation [13]:

$$G = \frac{I_{Ph}}{I_d} \quad (7)$$

Fig 6 shows the gain-voltage curves of the fabricated UV-sensor based on ZnO thin films. It shows that the maximum gain was obtained when the bias of 3.83V was applied. Therefore, the best performance of this device is in this potential value.

Fig 7 shows the consecutive current spectrum of fabricated UV-sensor under pulsed UV illumination. For this device, the photocurrent is increased to a saturation value upon illumination followed by a decrease when the light is switched off. The rise time is defined as the time taken for the sensor to reach 90% of its saturation current; while the recovery time refers to the time taken for the sensor to decrease its current from saturation to 10% of its saturation current value.

TABLE 1. The structural parameters of deposited ZnO thin film on the glass substrate

sample	Peak position (2θ)	*d*-spacing (Å)	a (Å)	c (Å)	(*hkl*)	D (nm)	FWHM (2θ)	Ref
ZnO thin film	34.28	2.613	3.070	5.227	(002)	44.5	0.38	this study
ZnO thin film	34.50	2.583	-	5.167	(002)	23.21	-	2

The photocurrent for the fabricated photodetector is highly stable and reproducible under pulsed UV illumination. The rise time and recovery time of fabricated photodetectors are presented in Table 2.

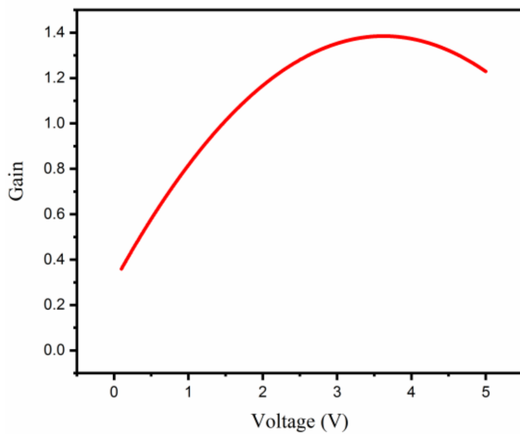

Figure 6. The gain-voltage curve of the fabricated UV-detector based on ZnO thin film

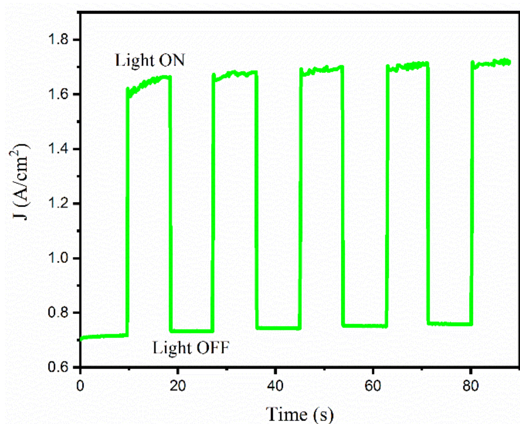

Figure 7. The consecutive current spectrum of fabricated UV-sensor under pulsed UV illumination

TABLE 2. The calculated photosensitivity and the speed of fabricated UV detector

Sample	Sensitivity	Rise time (s)	Recovery time (s)
ZnO pebbles	0.32	0.40	0.45

4. CONCLUSION

In summary, the ZnO thin films were deposited on a bare glass substrate using RF sputtering technique. The XRD patterns illustrated the hexagonal structure of deposited ZnO with the highly preferred orientation to (002) plane. The surface morphology of deposited films was uniform, smooth, and covered the surface substrate homogeneously without any cracks and pinholes on the surface. This sample indicated the high transmittance spectrum in the UV-VIS region. This sample did not show transmission in the ultraviolet region due to the optical bandgap (3.27 eV) of deposited ZnO thin films and the transmission cut-off at the wavelength of 387nm. The fabricated MSM photodetector based on Au/CdS indicated a short rise time of 0.40s and recovery time of 0.45s in pulsed UV illumination.

5. ACKNOWLEDGEMENTS

The present study was supported by Materials and Energy Research Center (MERC), Karaj, IRAN through Grant No. 99392008.

REFERENCES

1. Sang, L., Liao, M., Sumiya, M., "A comprehensive review of semiconductor ultraviolet photodetectors: from thin film to one-dimensional nanostructures", ***Sensors***, Vol. 13, No. 8, (2013), 10482-10518.
2. Daniel, G.P., Justinvictor, V.B., Nair, P.B., Joy, K., Koshy, P., Thomas, P.V., "Effect of annealing temperature on the structural and optical properties of ZnO thin films prepared by RF magnetron sputtering", ***Physica B: Condens Matter***, Vol. 405, No. 7, (2010), 1782-1786.
3. Purohit, A., Chander, S., Sharma, A., Nehra, S.P., Dhaka, M.S., "Impact of low temperature annealing on structural, optical, electrical and morphological properties of ZnO thin films grown by RF sputtering for photovoltaic applications", ***Optical Materials***, Vol. 49, (2015), 51-58.
4. Ondo-Ndong, R., Pascal-Delannoy, F., Boyer, A., Giani, A., Foucaran, A., "Structural properties of zinc oxide thin films prepared by rf magnetron sputtering", ***Materials Science and Engineering: B***, Vol. 97, No. 1, (2003), 68-73.
5. Liu, K., Sakurai, M., Aono, M., "ZnO-based ultraviolet photodetectors", Sensors, Vol. 10, No. 9, (2010), 8604-8634.
6. Kim, K.S., Kim, H.W., Kim, N.H., "Structural characterization of ZnO films grown on SiO_2 by the RF magnetron sputtering", ***Physica B: Condensed Matter***, Vol. 334, No. 3-4, (2003), 343-346.
7. Besleaga, C., Stan, G.E., Galca, A.C., Ion, L., Antohe, S., "Double layer structure of ZnO thin films deposited by RF-magnetron sputtering on glass substrate", ***Applied Surface Science***, Vol. 258, No. 22, (2012), 8819-8824.
8. Zhang, D.H., Xue, Z.Y., Wang, Q.P., "The mechanisms of blue emission from ZnO films deposited on glass substrate by rf magnetron sputtering", ***Journal of Physics D: Applied Physics***, Vol. 35, No. 21, (2002), 2837–2840.
9. Kumar, S., Sharma, P., Sharma., "Structural transition in II-VI nanofilms: Effect of molar ratio on structural, morphological, and optical properties", ***Journal of Applied Physics***, Vol. 111, No. 11, (2012), 113510.
10. Naderi, N., Hashim, M.R., "Nanocrystalline SiC sputtered on porous silicon substrate after annealing", ***Materials Letters***, Vol. 97, (2013), 90–92.

11. Kumar, V., Kumar, V., Som, S., Yousif, A., Singh, N., Ntwaeaborwa, O.M., Kapoor, A., Swart, H.C., "Effect of annealing on the structural, morphological and photoluminescence properties of ZnO thin films prepared by spin coating", ***Journal of Colloid and Interface Science***, Vol. 428, (2014), 8–15.
12. Barote, M.A., Yadav, A.A., Masumdar, E.U., "Synthesis, characterization and photoelectrochemical properties of n-CdS thin films", ***Physica B: Condensed Matter***, Vol. 406, No. 10, (2011), 1865–1871.
13. Moghaddam, M., Naderi, N., Hosseinifard, M., Kazemzadeh, A., "Improved optical and structural properties of cadmium sulfide nanostructures for optoelectronic applications", ***Ceramics International***, Vol. 46, No. 6, (2020), 7388-7395.